J Physiol 593.8 (2015) pp 1841–1856

The Journal of Physiology

Effects of lung ventilation–perfusion and muscle metabolism–perfusion heterogeneities on maximal O_2 transport and utilization

I. Cano[1,2], J. Roca[1,2] and P. D. Wagner[3]

[1] *Hospital Clinic, IDIBAPS, CIBERES, Universitat de Barcelona, Barcelona, Catalunya, Spain*
[2] *Centro de Investigación en Red de Enfermedades Respiratorias (CibeRes), Palma de Mallorca, Spain*
[3] *School of Medicine University of California, San Diego, San Diego, CA 92093-0623A, USA*

Key points

- We expanded a prior model of whole-body O_2 transport and utilization based on diffusive O_2 exchange in the lungs and tissues to additionally allow for both lung ventilation–perfusion and tissue metabolism–perfusion heterogeneities, in order to estimate $\dot{V}_{O_2}$ and mitochondrial P_{O_2} (P_{mO_2}) during maximal exercise.
- Simulations were performed using data from (a) healthy fit subjects exercising at sea level and at altitudes up to the equivalent of Mount Everest and (b) patients with mild and severe chronic obstructive pulmonary disease (COPD) exercising at sea level.
- Heterogeneity in skeletal muscle may affect maximal O_2 availability more than heterogeneity in lung, especially if mitochondrial metabolic capacity ($\dot{V}_{MAX}$) is only slightly higher than the potential to deliver O_2, but when $\dot{V}_{MAX}$ is substantially higher than O_2 delivery, the effect of muscle heterogeneity is comparable to that of lung heterogeneity.
- Skeletal muscle heterogeneity may result in a wide range of potential mitochondrial P_{O2} values, a range that becomes narrower as $\dot{V}_{MAX}$ increases; in regions with a low ratio of metabolic capacity to blood flow, P_{mO_2} can exceed that of mixed muscle venous blood.
- The combined effects of lung and peripheral heterogeneities on the resistance to O_2 flow in health decreases with altitude.

Abstract Previous models of O_2 transport and utilization in health considered diffusive exchange of O_2 in lung and muscle, but, reasonably, neglected functional heterogeneities in these tissues. However, in disease, disregarding such heterogeneities would not be justified. Here, pulmonary ventilation–perfusion and skeletal muscle metabolism–perfusion mismatching were added to a prior model of only diffusive exchange. Previously ignored O_2 exchange in non-exercising tissues was also included. We simulated maximal exercise in (a) healthy subjects at sea level and altitude, and (b) COPD patients at sea level, to assess the separate and combined effects of pulmonary and peripheral functional heterogeneities on overall muscle O_2 uptake ($\dot{V}_{O_2}$) and on mitochondrial P_{O_2} (P_{mO_2}). In healthy subjects at maximal exercise, the combined effects of pulmonary and peripheral heterogeneities reduced arterial P_{O_2} (P_{aO_2}) at sea level by 32 mmHg, but muscle $\dot{V}_{O_2}$ by only 122 ml min^{-1} (–3.5%). At the altitude of Mt Everest, lung and tissue heterogeneity together reduced P_{aO_2} by less than 1 mmHg and $\dot{V}_{O_2}$ by 32 ml min^{-1} (–2.4%). Skeletal muscle heterogeneity led to a wide range of potential P_{mO_2} among muscle regions, a range that becomes narrower as $\dot{V}_{MAX}$ increases, and in regions with a low ratio of metabolic capacity to blood flow, P_{mO_2} can exceed that of mixed muscle venous blood. For patients with severe COPD, peak $\dot{V}_{O_2}$ was insensitive to substantial changes in the mitochondrial characteristics for O_2 consumption or the extent of muscle heterogeneity. This integrative computational model of O_2 transport and utilization offers the potential for estimating profiles of P_{mO_2} both in health and in diseases

DOI: 10.1113/jphysiol.2014.286492

such as COPD if the extent for both lung ventilation–perfusion and tissue metabolism–perfusion heterogeneity is known.

(Resubmitted 29 October 2014; accepted after revision 27 January 2015; first published online 26 February 2015)
Corresponding author I. Cano: IDIBAPS, C/Villarroel 170, 08036, Barcelona, Spain. Email: iscano@clinic.ub.es

Abbreviations COPD, chronic obstructive pulmonary disease; DL, lung diffusing capacity; DM, tissue (muscle) diffusing capacity; [Hb], haemoglobin concentration; FEV, forced expired volume; F_{I,O_2}, inspired O_2 fraction; P_{aO_2}, arterial P_{O_2}; P_{mO_2}, mitochondrial P_{O_2}; $\dot{Q}$, blood flow distribution; $\dot{V}_A$, expired ventilation; $\dot{V}_A/\dot{Q}$, ventilation–perfusion inequality; $\dot{V}_I$, inspired ventilation; $\dot{V}_{O_2max}$, maximum oxygen delivery–uptake; $\dot{V}_{max}$, muscle metabolism; $\dot{V}_{MAX}$, mitochondrial maximal capacity for O_2 consumption.

Introduction

Current modelling of the O_2 pathway (Wagner, 1993, 1996; Cano *et al.* 2013) is based on the concept that it is the functional integration amongst all individual components of the oxygen transport and utilization system (i.e. lungs and chest wall, heart, blood and circulation, and tissue mitochondria) which determines maximal overall O_2 uptake ($\dot{V}_{O_2max}$). In these models, important simplifying assumptions were made. In particular, O_2 exchange within the lungs was simplified by ignoring ventilation–perfusion ($\dot{V}_A/\dot{Q}$) inequality, and exchange focused only on alveolar–capillary diffusion. This was felt to be reasonable as the minimal $\dot{V}_A/\dot{Q}$ inequality found in health (Wagner *et al.* 1974) is normally of minor importance to O_2 exchange, while allowing for such inequality greatly increased model complexity. However, this would be an unacceptable simplification in cardiopulmonary diseases where $\dot{V}_A/\dot{Q}$ inequality can be substantial. Similarly, within the muscles, potential heterogeneity of local metabolic capacity and demand ($\dot{V}_{O_2}$) in relation to blood flow distribution ($\dot{Q}$) was not considered, and while diffusive movement of O_2 from the muscle microcirculation to the mitochondria was modelled, the muscles were considered to be functionally homogeneous, i.e. with blood flow perfectly matched to O_2 demand throughout. Much less information exists about normal $\dot{V}_{O_2}/\dot{Q}$ heterogeneity in muscle (Richardson *et al.* 2001), but using near infrared spectroscopy (NIRS), preliminary data in normal subjects (Vogiatzis *et al.* 2015) suggest that $\dot{V}_{O_2}/\dot{Q}$ matching is much tighter than is $\dot{V}_A/\dot{Q}$ matching. Thus, $\dot{V}_{O_2}/\dot{Q}$ dispersion in muscle appears to be only about ¼ of $\dot{V}_A/\dot{Q}$ dispersion in normal lung (Wagner *et al.* 1987*a*,*b*).

Another simplifying assumption was that all of the cardiac output flowed to the exercising muscles, which is clearly untrue. This is not of great quantitative importance to muscle O_2 transport in health because of the ability to increase cardiac output to over 20 l min^{-1}, rendering the fraction of cardiac output perfusing non-exercising tissue small. However, such an assumption would pose a substantial limitation if the models were applied to patients with chronic cardiorespiratory disease where peak exercise may elicit less than a doubling of the resting cardiac output and resting $\dot{V}_{O_2}$.

The purpose of the study reported in the current paper was therefore to first expand the prior O_2 transport pathway model (Wagner, 1993, 1996; Cano *et al.* 2013) by allowing for (a) $\dot{V}_A/\dot{Q}$ heterogeneity in the lung, (b) $\dot{V}_{O_2}/\dot{Q}$ heterogeneity in the muscle, and (c) perfusion and metabolism in non-exercising tissues, and then to analyse the impact of possible heterogeneity in lungs and in peripheral exercising tissues, separately and combined, on overall O_2 transport and utilization at maximum exercise, both in health and in disease. In health, we simulated exercise not just at sea level but at altitudes up to the summit of Mt Everest using as input data variables obtained in Operation Everest II (Sutton *et al.* 1988). In disease, we chose COPD as the example of pulmonary gas exchange heterogeneity because of availability of O_2 transport data (Blanco *et al.* 2010), and because of general interest in muscle function in this disease.

We then posed four questions: (a) in health, what are the potential effects of lung and muscle heterogeneity (each modelled over a wide range) on oxygen flux and partial pressures at all steps in the O_2 pathway at sea level; (b) what is the impact of typical normal levels of heterogeneity on these variables when O_2 availability is reduced by exposure to high altitude; (c) how substantial variations of the three least well established determinants of O_2 flux and partial pressures in the transport–utilization pathway ($\dot{V}_{MAX}$ and P_{50} of the mitochondrial respiration curve and the extent of muscle heterogeneity) would affect both $\dot{V}_{O_2}$ and mitochondrial P_{O_2} estimates; and (d) what is the effect of (measured) lung and possible muscle heterogeneity on overall oxygen uptake and mitochondrial P_{O_2} in mild and severe COPD, where O_2 transport is less than normal.

Methods

The prior O_2 transport and utilization model

In the absence of heterogeneity in lungs or tissues, and ignoring metabolism and blood flow to non-exercising tissues, the system describing maximal O_2 transport and

utilization (Wagner, 1993, 1996; Cano *et al.* 2013) was composed of five mass conservation equations as shown in Fig. 1, which is reproduced from Cano *et al.* (2013) for the convenience of the reader. These equations represent: (1) O_2 transport by ventilation from the atmosphere to alveolar gas (eqn (1) in Fig. 1); (2) O_2 diffusion from the alveolar gas to the lung capillaries (eqn (2) in Fig. 1); (3) O_2 transport through the systemic circulation (eqn (3) in Fig. 1); (4) O_2 diffusion from systemic capillary blood to the muscle mitochondria (eqn (4) in Fig. 1); and (5) mitochondrial O_2 utilization (eqn (5) in Fig. 1).

The inputs to these equations are, at maximal exercise: inspired O_2 fraction (F_{I,O_2}), ventilation ($\dot{V}_I$, inspired; $\dot{V}_A$, expired), lung diffusing capacity (DL), cardiac output ($\dot{Q}$), acid–base status, haemoglobin concentration ([Hb]), tissue (muscle) diffusing capacity (DM) and the characteristics of mitochondrial respiration (modelled as a hyperbolic curve with its two parameters, $\dot{V}_{MAX}$ and P_{50}, as defined below and illustrated in Fig. 2). The five outputs, or unknowns, in these equations are the maximal rate of O_2 uptake ($\dot{V}_{O_2max}$) and alveolar, systemic arterial, venous and mitochondrial P_{O_2} values.

While the focus is clearly on O_2 transport, CO_2 cannot be ignored in such a model because of the effects of CO_2 retention, for example on the O_2Hb dissociation curve and on alveolar P_{O_2}. Thus, the same processes and equations are used for CO_2, (West, 1971), treating CO_2 at every step side by side with O_2 using the published CO_2 dissociation curves and acid–base relationships based on Kelman's subroutines (Kelman, 1966) such that O_2–CO_2 interactions are accounted for both in the lungs and muscle. Furthermore, the effect of alveolar ventilation on arterial P_{CO_2} is also innately included as one of the input variables needed is total ventilation. An exception is made for mitochondrial respiration, where, because the mitochondrial respiration curve for O_2 consumption does not apply to CO_2, CO_2 production is related to $\dot{V}_{O_2}$ through a stipulated value of the respiratory quotient, and the solutions for both gases sought simultaneously.

Modelling lung ventilation–perfusion inequality

To expand the model and allow for ventilation–perfusion ($\dot{V}_A/\dot{Q}$) inequality, ventilation and perfusion within the lung were distributed amongst a set of virtual lung compartments, each defined by its own ratio of ventilation ($\dot{V}_A$) to blood flow ($\dot{Q}$), with the compartments connected in parallel. This is exactly the same approach as first advanced by West in 1969 (West, 1969). Then, the computation for diffusive alveolar–capillary exchange, previously applied to just a single lung compartment representing the homogeneous lung, is now applied to all

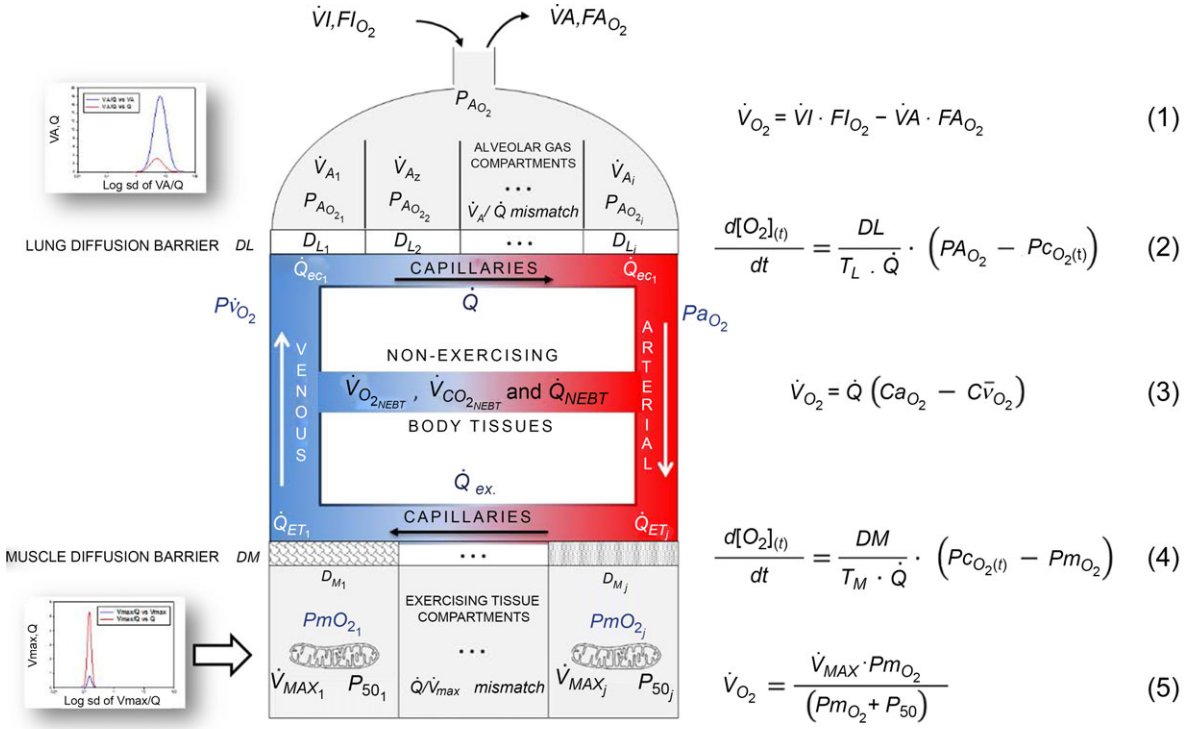

Figure 1. Schematic representation of the oxygen transport and utilization system
The schematic representation is shown with the five associated mass conservation equations governing O_2 transport (eqns (1)–(4)) and utilization (eqn (5)). Reproduced from Cano *et al.* (2013) with permission.

compartments in turn. The entering mixed venous blood is the same for all compartments, and the task is to compute the P_{O_2} and P_{CO_2} values expected at the end of the capillary in each compartment of different $\dot{V}_A/\dot{Q}$ ratio. This is done with a forward numerical integration procedure (Wagner *et al.* 1974), also used in Cano *et al.* (2013), and the outcome for each compartment depends on the compartmental DL/$\dot{Q}$ and $\dot{V}_A/\dot{Q}$ ratios, the inspired gas and mixed venous blood O_2 and CO_2 composition, and the shape and position of the respective binding curves in blood. This approach is in fact the same as developed by Hammond & Hempleman (1987), and which is also contained within the multiple inert gas elimination technique (Wagner, 2008). Once all compartments have been subjected to this numerical integration, O_2 and CO_2 concentrations in their effluent blood are averaged in a perfusion-weighted manner to compute the O_2 and CO_2 profile of the systemic arterial blood that will reach both the exercising muscles and non-exercising tissues and organs.

In the present application, two means of data entry are possible for specifying the features of the $\dot{V}_A/\dot{Q}$ distribution, allowing flexibility. Individual compartmental values for ventilation and blood flow can be used, or the compartments can be calculated based on a $\dot{V}_A/\dot{Q}$ distribution containing one or more modes, using for each mode its first three moments (mean, dispersion and skewness) as originally programmed by West (1969). Both types of inputs end up providing a multi-compartmental $\dot{V}_A/\dot{Q}$ distribution (indicated in Fig. 1). For simplicity, when computing the lung compartments based on a $\dot{V}_A/\dot{Q}$ distribution, the lung diffusing capacity (DL) was always distributed in proportion to compartmental blood flow, so that compartmental DL/$\dot{Q}$ remains constant throughout the lung. This decision does not eliminate the opportunity to introduce actual data on DL/$\dot{Q}$ distribution when available.

In summary, to allow for $\dot{V}_A/\dot{Q}$ heterogeneity, the single homogeneous lung 'compartment' in the prior model has been replaced by a multi-compartment model built from the algorithms of West (1969) as modified by Hammond & Hempleman (1987) and which allows for both $\dot{V}_A/\dot{Q}$ inequality and diffusive exchange. Just as in the prior model, necessary inputs remain the composition of inspired gas and mixed venous blood, and the output remains the composition of systemic arterial blood destined for the muscles and other tissues.

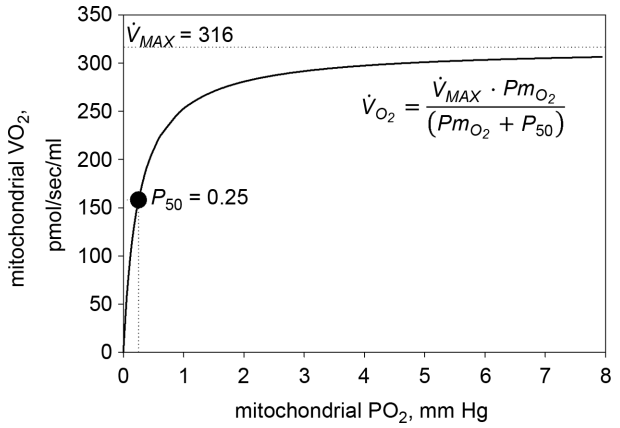

Figure 2. Graphical depiction of the hyperbolic equation for oxidative phosphorylation
The graphical depiction of the equation for oxidative phosphorylation (eqn (1) in Fig. 1) is fitted to data of Scandurra & Gnaiger (2010; p. 16, Fig 3*B*).

Modelling peripheral heterogeneity

Similarly to lung ventilation–perfusion mismatch, tissue heterogeneities are considered as (regional) variability in a functional ratio. However, instead of $\dot{V}_A/\dot{Q}$ being that ratio as in the lung, it is the ratio of mitochondrial metabolic capacity ($\dot{V}_{MAX}$) to blood flow ($\dot{Q}$) that is considered in the muscles. Here, $\dot{V}_{MAX}$ is the local mitochondrial maximal metabolic capacity to use O_2, and is the very same parameter as $\dot{V}_{MAX}$ in eqn (5), Fig. 1. The ratio $\dot{V}_{MAX}/\dot{Q}$ in essence expresses the balance between O_2 supply ($\dot{Q}$) and O_2 demand ($\dot{V}_{MAX}$). In the prior model, the muscle was considered homogeneous in terms of $\dot{V}_{MAX}/\dot{Q}$ ratios, but now the muscle is considered as a parallel collection of muscle 'units' each with its own ratio of $\dot{V}_{MAX}/\dot{Q}$. Exactly as with the lung, the $\dot{V}_{MAX}/\dot{Q}$ distribution can be specified either as a set of individual compartmental values for $\dot{Q}$, DM, $\dot{V}_{MAX}$ and P_{50}, or computed from the moments of a (multimodal) $\dot{V}_{MAX}/\dot{Q}$ distribution. While it would be possible to assign every $\dot{V}_{MAX}/\dot{Q}$ compartment a unique mitochondrial P_{50} (see eqn (5) in Fig. 1), this has not been modelled to date, and P_{50} has been taken to be constant throughout any single muscle. Also as in the lung, diffusion is considered in every $\dot{V}_{MAX}/\dot{Q}$ unit, with the diffusing capacity DM distributed in proportion to $\dot{Q}$, just as for the lung. However, the algorithm can accommodate different values across compartments for both P_{50} and DM if desired. The same forward integration procedure is used as in the prior model (Cano *et al.* 2013), when it was applied to the entire muscle considered as one homogeneous unit to compute each muscle compartment's effluent venous O_2 and CO_2 levels for the given inflowing arterial blood composition, and the $\dot{V}_{MAX}/\dot{Q}$ and DM/$\dot{Q}$ ratios of the unit. Again as in the lung, the effluent venous blood from all muscle units is combined, or mixed, in terms of both O_2 and CO_2 concentrations, and a resulting mixed muscle venous P_{O_2} and P_{CO_2} is then calculated. Finally, this blood is mixed with that from the non-exercising tissues (see

below). This mixed venous blood returns to the lungs for re-oxygenation.

In summary, to allow for $\dot{V}_{MAX}/\dot{Q}$ heterogeneity, the single homogeneous muscle 'compartment' in the prior model has been replaced by a multi-compartment model which allows for both $\dot{V}_{MAX}/\dot{Q}$ inequality and diffusion impairment. Similarly to the prior model, necessary additional inputs remain the composition of arterial blood, and the blood binding characteristics of O_2 and CO_2. The output remains the composition of mixed muscle venous blood destined for return to the lungs for re-oxygenation.

In this section, the expression of peripheral heterogeneity using the oxygen flow ($\dot{Q}_{O_2}$) instead of blood flow ($\dot{Q}$) was considered, but since at any given arterial P_{O_2}, the arterial blood entering any muscle region has the same oxygenation, the distribution of $\dot{V}_{MAX}/\dot{Q}$ will not differ in dispersion from that of $\dot{V}_{MAX}/\dot{Q}$ delivery. Moreover, O_2 concentration is an outcome variable. Hence, we cannot in practice adopt O_2 delivery as the denominator.

Modelling metabolism and blood flow to non-exercising tissues

Non-exercising tissue blood flow and metabolism are incorporated simply by assigning values for total non-exercising tissue $\dot{V}_{O_2}$ and $\dot{Q}$, and using the Fick principle to compute the tissue venous O_2 concentration. Then, a mixing equation combines venous blood from this non-exercising tissue with that from the mixed muscle venous blood (see above) in proportion to the blood flow rates assigned to the non-exercising tissues and muscles respectively, to form what will be pulmonary arterial blood reaching the lungs for re-oxygenation.

Achieving a solution for the model

In the prior model it was explained (Cano *et al.* 2013) how the model was run and a solution achieved. The same process is used with the above-described expansions in the current paper. In brief, a starting estimate is made for the composition of mixed venous blood entering the lungs, and for that estimate, the lung component is executed over the many $\dot{V}_A/\dot{Q}$ compartments and the end-capillary O_2 and CO_2 concentrations averaged over all compartments (weighted by compartmental blood flow) to yield an estimate of systemic arterial P_{O_2} and P_{CO_2}. These are then used as input data for the muscle part of the system, and that component is run once for each $\dot{V}_{MAX}/\dot{Q}$ compartment. The effluent compartmental venous O_2 and CO_2 levels are then averaged (again blood flow-weighted), and mixed with the blood draining the non-exercising tissues (see previous section). It is the P_{O_2} and P_{CO_2} of this mixed blood that is the new estimate at mixed venous P_{O_2} and P_{CO_2} for the next iteration (or cycle) of pulmonary gas exchange: To this point, all that has changed between the first and second cycles is the composition of mixed venous blood. After pulmonary gas exchange calculations using this new venous blood composition are complete, new values of arterial blood P_{O_2} and P_{CO_2} are calculated, and now muscle O_2 exchange is recomputed, from which new values of mixed venous P_{O_2} and P_{CO_2} are calculated. This cycling back and forth between the lungs and the tissues is continued until the five $\dot{V}_{O_2}$ estimates – one computed from each of the five equations in Fig. 1 – are identical (to within ± 0.1 ml min^{-1}). At this point, stability of all P_{O_2} values (alveolar, arterial, muscle venous and mitochondrial) in the face of further cycling between the lungs and tissues is also achieved. When this is observed, the governing requirement for conservation of mass has been achieved, and this signals the end of the run.

Analysis and input data for simulations

As mentioned above, four questions were posed, and these are discussed below.

First, in health, we assessed the effects of a wide range of lung and tissue functional heterogeneities on oxygen tensions and utilization at all steps of the O_2 pathway. This extensive exploration was carried out for conditions of maximal exercise breathing room air at sea level. To this end, input data defining O_2 transport conductances (i.e. ventilation, cardiac output, lung and muscle diffusional conductances) from normal subjects exercising maximally at sea level in Operation Everest II (Sutton *et al.* 1988) were used just as for the previous models (Wagner, 1993, 1996). Lung heterogeneity was analysed from complete homogeneity (logSD $\dot{Q} = 0$, second moment of the blood flow ($\dot{Q}$) distribution on a logarithmic $\dot{V}_A/\dot{Q}$ scale equals zero), to very high inhomogeneity (logSD $\dot{Q} = 2$) as might be seen in the critically ill. We also explored the effects of skeletal muscle heterogeneity on overall O_2 uptake ($\dot{V}_{O_2max}$) using a similar wide range of logSD $\dot{V}_{max}$ (second moment of the muscle metabolism ($\dot{V}_{max}$) distribution on a logarithmic $\dot{V}_{max}/\dot{Q}$ scale equals zero) from 0 to 2. The effects of lung and skeletal muscle heterogeneity on oxygen transport and utilization are displayed in Figs 3 and 4. In Fig. 3, and the first section in Results, the impact of skeletal muscle heterogeneity on $\dot{V}_{O_2max}$ is assessed at two different levels of $\dot{V}_{max}$ corresponding to 120% and 250% $\dot{V}_{O_2max}$.

The rationale behind a value for $\dot{V}_{max}$ of 4.6 l min^{-1}, which is 20% higher than the measured $\dot{V}_{O_2max}$ (3.8 l min^{-1}) at sea level in Operation Everest II (Sutton *et al.* 1988), is that it is a conservative estimate. This is so, because it is known that measured $\dot{V}_{O_2max}$ is less than mitochondrial capacity to use O_2 (i.e. $\dot{V}_{max}$) in healthy

fit subjects and exercise capacity is known to be increased within this range when breathing 100% O_2 (Welch, 1982; Knight *et al.* 1992).

However, we acknowledge that reports on subjects exercising a limited amount of muscle mass, (i.e. knee extensor of one limb); Andersen & Saltin, 1985) indicate the potential for markedly higher $\dot{V}_{max}$ values up to 250% of $\dot{V}_{O_2max}$ (which would scale to 9.5 l min^{-1} for $\dot{V}_{O_2max}$ measured in subjects from Operation Everest II). In the study by Andersen & Saltin, a rate of 350 ml kg^{-1} was measured, which extrapolated to a conservative estimate of 27 kg of exercising muscle mass corresponds to a $\dot{V}_{O_2max}$ value of 9.5 l min^{-1}. Consequently, these two $\dot{V}_{max}$ values (4.6 and 9.5 l min^{-1}) were used for the simulations displayed in Fig. 3.

For the mitochondrial P_{50}, we used a value of 0.3 mmHg, similar to what has been found experimentally *in vitro* (Wilson *et al.* 1977; Gnaiger *et al.* 1998; Scandurra & Gnaiger, 2010).

For non-exercising body tissues we used typical resting total values of $\dot{V}_{O_2}$ (300 ml min^{-1}), $\dot{V}_{CO_2}$ (240 ml min^{-1}) and blood flow (20% of total blood flow at peak exercise).

The second question examined the effects of heterogeneity in healthy lungs and muscle on O_2 transport and utilization at altitude. For the lung we used logSD $\dot{Q} = 0.5$ as a value commonly seen during exercise (Wagner *et al.* 1987*a*,*b*). This value is near the upper end of the normal range, which is 0.3–0.6 (Wagner *et al.* 1987*a*,*b*). In muscle, we used preliminary unpublished estimates of logSD $\dot{V}_{max} = 0.1$. Again for P_{50}, we used a value of 0.3 mmHg and for $\dot{V}_{max}$ we used a conservative value 20% higher than the measured $\dot{V}_{O_2max}$. The input data defining the O_2 transport conductances again came from normal subjects exercising maximally at sea level and altitude in Operation Everest II (Sutton *et al.* 1988) as used above and again typical resting total values of $\dot{V}_{O_2}$ (300 ml min^{-1}), $\dot{V}_{CO_2}$ (240 ml min^{-1}) and blood flow (20% of total blood flow at peak exercise) were considered for non-exercising body tissues. However, to study the consequences at more altitudes than were examined in Operation Everest II (which were sea level, 4600 m, 6100 m, 7600 m and 8848 m), O_2 transport conductance parameters were linearly interpolated (Table 1) at 305 m (1000 ft) elevation increments from the data obtained at each of the five altitudes studied in Operation Everest II (Sutton *et al.* 1988).

For the third and forth questions we assessed how substantial variations of the three least well established determinants of O_2 flux and partial pressures in the transport–utilization pathway ($\dot{V}_{MAX}$ and P_{50} of the mitochondrial respiration curve and logSD $\dot{V}_{MAX}$) would affect both $\dot{V}_{O_2}$ and mitochondrial P_{O_2} estimates, in health (third question) and in COPD (fourth question). Input data defining O_2 transport conductances and lung heterogeneity (i.e. logSD $\dot{Q} = 0.5$) from normal subjects exercising maximally at sea level in Operation Everest II

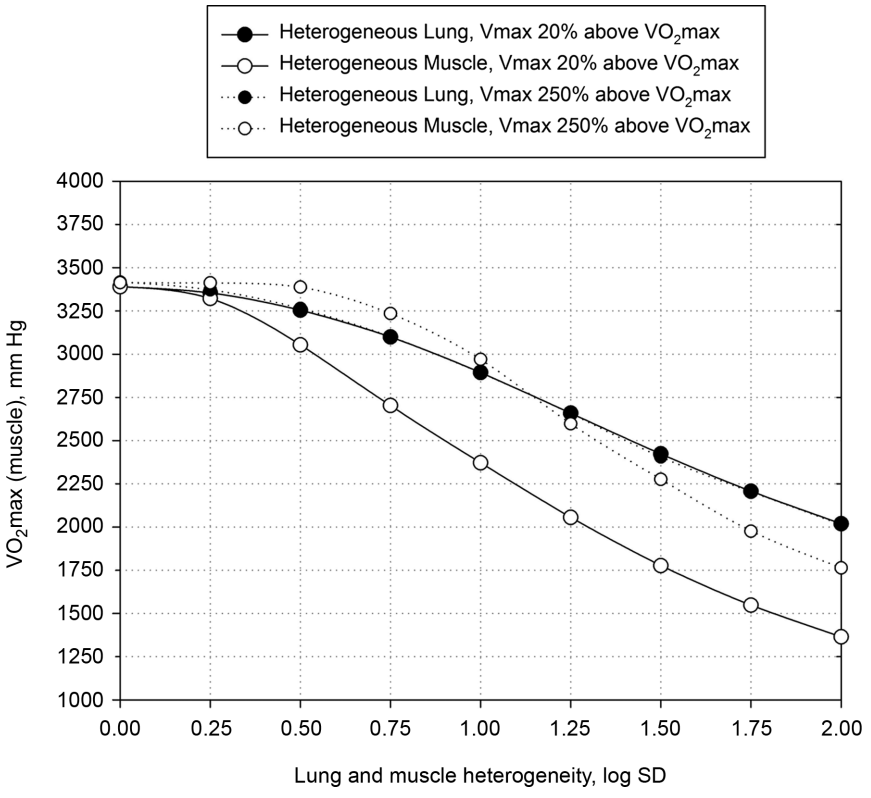

Figure 3. Effects of potential lung and muscle heterogeneities on maximal O_2 transport and utilization
Independent effects of lung $\dot{V}_A/\dot{Q}$ heterogeneity (filled circles) and muscle $\dot{V}_{MAX}/\dot{Q}$ heterogeneity (open circles) on maximal muscle oxygen uptake ($\dot{V}_{O_2max}$), using input data defining O_2 transport conductances from normal subjects exercising maximally at sea level in Operation Everest II (Sutton *et al.* 1988). Results shown for $\dot{V}_{MAX}$ 20% higher than measured $\dot{V}_{O_2max}$ (continuous line) and $\dot{V}_{MAX}$ 2.5-fold higher than measured $\dot{V}_{O_2max}$ (dotted line). Healthy subjects show pulmonary logSD $\dot{Q}$ between 0.3 and 0.6 (Wagner *et al.* 1974), whereas skeletal muscle heterogeneity (logSD $\dot{V}_{MAX}$) presents an average value of 0.10 (Vogiatzis *et al.* 2015). In patients with moderate to severe COPD, logSD $\dot{Q}$ can present values close to 1.0, but no published data on logSD $\dot{V}_{MAX}$ are available. Finally, critically ill patients admitted in the Intensive Care Unit (ICU) may show lung heterogeneity values close to 2.0. Again, no information on logSD $\dot{V}_{MAX}$ is available.

Table 1. Input parameters for the modelling of the oxygen transport system in health at sea level and altitude

Altitude (ft)	Barometric pressure (P_B; mmHg)	Body temperature (T; °C)	Haemoglobin concentration ([Hb]; g dl^{-1})	Alveolar ventilation ($\dot{V}$ (BTPS); l min^{-1})	Blood flow ($\dot{Q}$; l min^{-1})	Total lung O_2 diffusing capacity (DL; ml min^{-1} mmHg^{-1})	Total muscle O_2 diffusing capacity (DM; ml min^{-1} mmHg^{-1})
0	760	38	14.2	128.3	25.0	50.9	104.6
5000	639	38	14.9	137.1	23.5	60.9	97.1
10,000	534	38	15.5	145.9	22.0	70.9	89.6
15,000	442	38	16.2	154.6	20.5	80.9	82.1
16,000	426	37.9	16.3	156.4	20.2	82.9	80.6
17,000	410	37.8	16.5	158.1	19.9	84.9	79.1
18,000	394	37.7	16.6	159.9	19.6	86.9	77.6
19,000	380	37.6	16.7	161.6	19.3	88.9	76.1
20,000	365	37.5	16.9	163.4	19.0	90.9	74.6
21,000	351	37.4	17.0	165.2	18.7	92.9	73.1
22,000	337	37.3	17.1	166.9	18.4	94.9	71.6
23,000	324	37.2	17.2	168.7	18.1	96.9	70.1
24,000	311	37.1	17.4	170.4	17.8	98.9	68.6
25,000	299	37	17.5	172.2	17.5	100.9	67.1
26,000	286	37	17.6	173.9	17.2	102.9	65.6
27,000	275	37	17.8	175.7	16.9	104.9	64.1
28,000	264	37	17.9	177.4	16.6	106.9	62.6
29,000	253	37	18.0	179.2	16.3	108.9	61.1
30,000	243	37	18.2	181.0	16.0	110.9	59.6

(Sutton *et al.* 1988) were used in health. In disease, measured O_2 conductances and lung heterogeneity data came from two previously studied COPD patients (Blanco *et al.* 2010) exercising maximally (Table 2), one with mild (FEV_1 = 66% predicted post-bronchodilator) and one with severe (FEV_1 = 23% predicted post-bronchodilator) COPD. However, even if reasonable, the values of $\dot{V}_{MAX}$and P_{50} assumed to answer the previous question are uncertain, let alone whether there is significant $\dot{V}_{MAX}/\dot{Q}$ heterogeneity. Because of this, we carried out simulations over a wide range of possible values of these variables, as indicated in Fig. 6. In the case of $\dot{V}_{max}$, we used a values of 4.2, 4.6 and 4.9 l min^{-1} (10, 20% and 30% higher than actual $\dot{V}_{O_2max}$, respectively). Moreover, a $\dot{V}_{max}$ value of 9.5 l min^{-1} (250% $\dot{V}_{O_2max}$) was also considered in health because of the rationale described above.

For mitochondrial P_{50}, we used values lower (0.14 mmHg) and higher (0.46 mmHg) than 0.3 mmHg, the value found experimentally *in vitro* (Wilson *et al.* 1977; Gnaiger *et al.* 1998; Scandurra & Gnaiger, 2010). Finally, to assess how sensitive the outcomes are to the degree of heterogeneity, we also carried out calculations with logSD $\dot{V}_{MAX}$ values of 0.1 (healthy subject estimates), 0.2 and 0.3. With respect to non-exercising body tissues, we used typical resting total values of $\dot{V}_{O_2}$ (300 ml min^{-1}), $\dot{V}_{CO_2}$ (240 ml min^{-1}) and blood flow (20% of total blood flow at peak exercise) for normal subjects.

For the two previously studied COPD patients (Blanco *et al.* 2010) exercising maximally we used measured resting values of whole body $\dot{V}_{O_2}$ ($\dot{V}_{O_2rest}$ and $\dot{V}_{CO_2}$ (Table 2), along with a blood flow estimate ($\dot{Q}_{non-exercising}$) from the following formula, which expresses the concept that blood flow is proportional to metabolic rate: $\dot{Q}_{non-exercising} = \dot{Q}_{max}\left(\dot{V}_{O_2rest}/\dot{V}_{O_2\,max}\right)$.

Results

Effects of potential lung and muscle heterogeneities on O_2 transport and utilization in healthy subjects exercising maximally at sea level

Figure 3 shows the independent effects of lung $\dot{V}_A/\dot{Q}$ heterogeneity (filled circles) and muscle $\dot{V}_{MAX}/\dot{Q}$ heterogeneity (open circles) on maximal muscle oxygen uptake ($\dot{V}_{O_2max}$), in normal subjects exercising maximally at sea level. In this figure, both $\dot{V}_A/\dot{Q}$ and $\dot{V}_{MAX}/\dot{Q}$ heterogeneity has been varied over a wide range of log SD, from 0 to 2.0. Healthy subjects show pulmonary logSD $\dot{Q}$ between 0.30 and 0.60 (Wagner *et al.* 1987*a*), whereas skeletal muscle heterogeneity (logSD $\dot{V}_{max}/\dot{Q}$) presents an average value of 0.10 (Vogiatzis *et al.* 2015). In patients with moderate to severe COPD, logSD $\dot{Q}$ can present values close to 1.0, but no published data on logSD $V_{max}/\dot{Q}$ are available. Finally, critically ill patients admitted in the Intensive Care Unit (ICU) may show lung heterogeneity values close to 2.0, but no information on logSD $\dot{V}_{max}/\dot{Q}$ is available. The main result from Fig. 3 is that heterogeneity in muscle affects O_2 availability

Table 2. Input parameters for the modelling of the oxygen transport system in disease (moderate and severe COPD)

Parameter	Moderately limited transport	Severely limited transport
Forced expired volume in the 1st second (FEV_1; % predicted post-bronchodilator)	66	23
Forced vital capacity (FVC; % predicted post-bronchodilator)	84	33
FEV_1/FVC	0.58	0.54
Log SD $\dot{Q}$	0.67	0.86
Barometric pressure (P_B; mmHg)	758	765
Fractional inspired oxygen (F_{I,O_2})	0.2093	0.2093
Haemoglobin concentration ([Hb]; g dl^{-1})	14.4	12.5
O_2 dissociation curve (P_{50}; mmHg)	26.8	26.8
Body temperature (T; °C)	37.0	36.8
Weight (kg)	60	36
Body mass index (BMI; kg m^{-2})	19.8	15.2
Resting ventilation ($\dot{V}$ (BTPS); l min^{-1})	7.11	7.44
Resting cardiac output ($\dot{Q}$; l min^{-1})	3.68	3.20
Resting $\dot{V}_{O_2}$(ml min^{-1})	235	159
Resting $\dot{V}_{CO_2}$ (ml min^{-1})	174	103
Resting arterial P_{O_2} (P_{aO_2}; mmHg)	80	59
Resting arterial P_{CO_2} (P_{aCO_2}; mmHg)	35	46
Resting lactate (mmol l^{-1})	1.47	0.81
Exercise ventilation ($\dot{V}$ (BTPS); l min^{-1})	35.3	8.2
Exercise cardiac output ($\dot{Q}$; l min^{-1})	7.87	3.98
Exercise ($\dot{V}_{O_2}$; ml·min^{-1})	914	355
Exercise arterial P_{O_2} (P_{aO_2}; mmHg)	90	59
Exercise arterial P_{CO_2} (P_{aCO_2}; mmHg)	31	49
Exercise lung O_2 diffusing capacity (DL; ml min^{-1} $mmHg^{-1}$)	100	11
Exercise muscle O_2 diffusing capacity (DM; ml min^{-1}·$mmHg^{-1}$)	26	9
Exercise lactate (mmol l^{-1})	3.55	2.03

more than does heterogeneity in the lungs if $\dot{V}_{MAX}$ is only 20% higher than $\dot{V}_{O_2max}$. However, using the higher $\dot{V}_{MAX}$ (i.e. 9.5 l min^{-1}), the effects of lung and muscle heterogeneity are similar. On the other hand, the impact of lung heterogeneity on $\dot{V}_{O_2max}$ is insensitive to the $\dot{V}_{MAX}$ values used. In addition, because muscle heterogeneity appears to be much less than that in the lung, both in health and COPD, based on a combination of published and unpublished data as mentioned, actual muscle heterogeneity has less of an impact on O_2 transport than observed lung heterogeneity.

The six panels in Fig. 4 display the estimated (combined and separate) effects of lung and muscle heterogeneities on the O_2 transport and utilization system. The upper-left panel indicates arterial P_{O_2} (P_{aO_2}) over a range of exercising muscle $\dot{V}_{MAX}/\dot{Q}$ mismatching (0 to 0.5), expressed as logSD $\dot{V}_{max}$. For each logSD V_{max} value, the panel displays P_{aO_2} values for different levels of lung $\dot{V}_A/\dot{Q}$ heterogeneity, from the homogeneous lung logSD $\dot{Q} = 0$) to a highly heterogeneous lung (logSD $\dot{Q} = 2$). Each line represents the outcome at a given level of lung heterogeneity over a range of muscle heterogeneity. This panel shows that muscle heterogeneity has only a small effect on P_{aO_2} at all levels of lung functional heterogeneities. However, as is well known, $\dot{V}_A/\dot{Q}$ inequality has a major impact on arterial oxygenation as shown. Likewise, the upper-right panel shows the effects of muscle heterogeneity on effluent muscle venous P_{O_2} (P_{vO_2}). The impact is moderate, and is greater than the effect on P_{aO_2}. However, it is quantitatively important only at high levels of tissue heterogeneity, especially in combination with lungs containing little heterogeneity.

The two middle panels of Fig. 4 show the relationships between mitochondrial P_{O_2} (P_{mO_2}) among muscle regions (compartments) and skeletal muscle $\dot{V}_{MAX}/\dot{Q}$ functional heterogeneity. The left hand panel shows the lowest compartmental values of P_{mO_2} (i.e. when $\dot{V}_{MAX}/\dot{Q}$ is high) and the right hand panel shows the highest compartmental values of P_{mO_2} (i.e. when $\dot{V}_{MAX}/\dot{Q}$ is low). Note that the ordinate scales are very different in these two panels. These panels show that heterogeneity of $\dot{V}_{MAX}/\dot{Q}$ ratios markedly expands the range of P_{mO_2} levels among exercising skeletal muscle compartments. As in the top panels, each line in the two middle panels correspond to different levels of lung heterogeneity from a homogeneous lung (logSD $\dot{Q} = 0$) to a highly heterogeneous lung (logSD $\dot{Q} = 2$).

The left middle panel shows that, as expected, the greater the peripheral heterogeneity, the lower the minimum P_{mO_2} values. Moreover, we observe a moderate impact of lung heterogeneity on minimum P_{mO_2}, but such impact decreases as skeletal muscle heterogeneity increases. Likewise, the right middle panel shows that skeletal muscle compartments with lowest $\dot{V}_{MAX}/\dot{Q}$ ratios may generate exceedingly high P_{mO_2} estimates that increase with tissue heterogeneity. Homogeneous lungs show the highest P_{mO_2} values for a given level of peripheral tissue functional heterogeneity.

The lower left panel indicates that muscle heterogeneities have small effects on total muscle $\dot{V}_{O_2}$, especially compared with lung heterogeneities that show

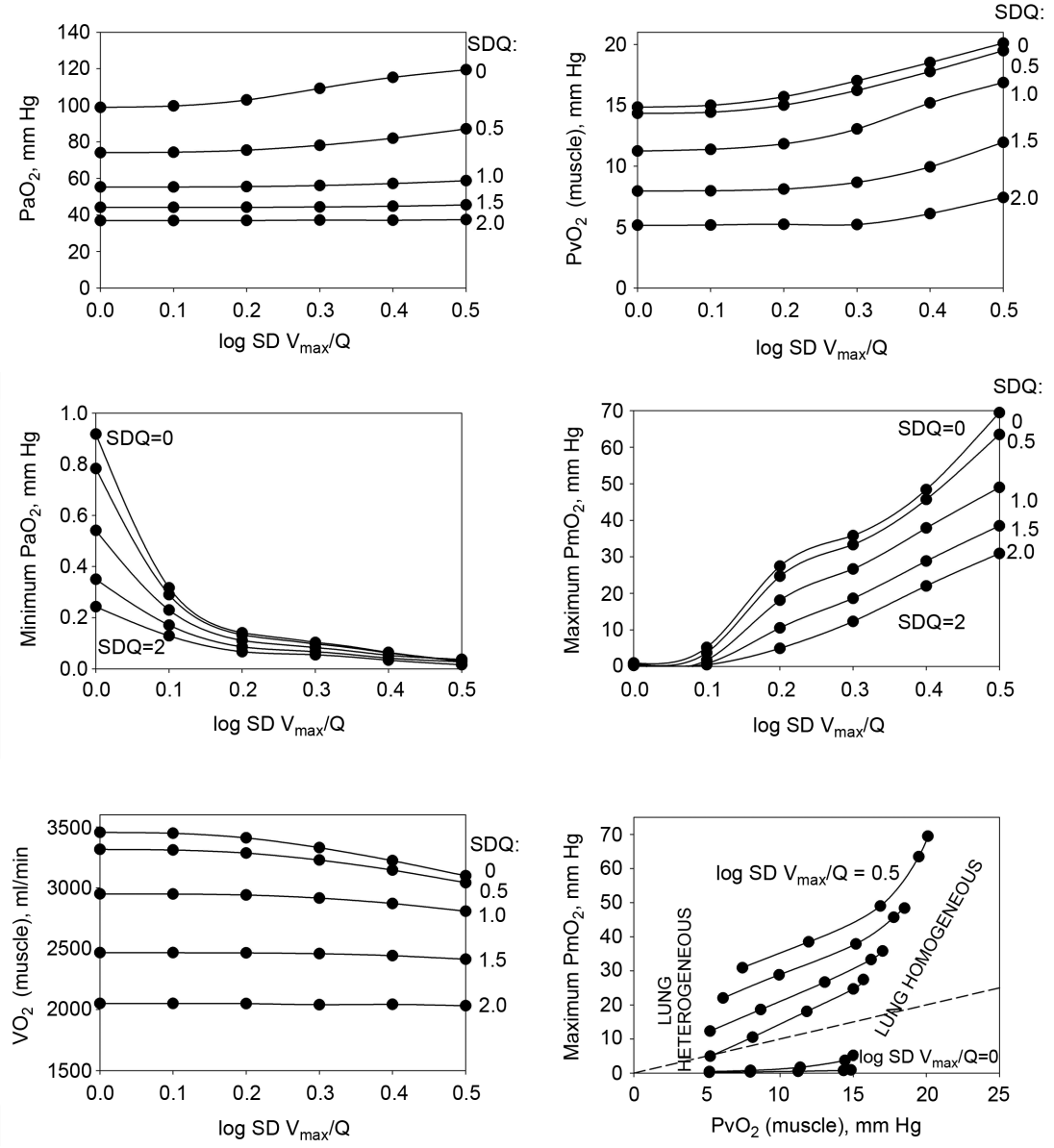

Figure 4. Combined and separate effects of lung and muscle heterogeneities on the O_2 transport and utilization system
Combined and separated effects of varying degrees of lung ventilation–perfusion heterogeneity (SDQ) and varying degrees of exercising muscle mitochondrial metabolic capacity–blood flow heterogeneities (logSD $\dot{V}_{MAX}$) on the O_2 transport pathway: P_{O_2} on arterial blood (upper left panel), venous blood (upper right panel) and mitochondria (two central panels), maximal muscle oxygen uptake (lower left panel), and, maximum degree of oxygen unbalance between mitochondrial ($P_{m_{O_2}}$) of muscle compartments and mean effluent venous ($P_{v_{O_2}}$) oxygen levels (lower-right panel). See text for details.

a significant impact on muscle $\dot{V}_{O_2max}$. Finally, the lower right panel displays the maximum estimates for P_{mO_2} among muscle regions (as seen in the middle right panel of the same figure) plotted against the corresponding mean effluent muscle P_{vO_2} (from the top right panel). The individual lines indicate different levels of muscle heterogeneities, from a homogeneous tissue (logSD $\dot{V}_{max}/\dot{Q} = 0$) at the bottom to heterogeneous muscle (logSD $\dot{V}_{max}/\dot{Q} = 0.5$) at the top. In the panel, the dashed straight line corresponds to the identity line. The point of presenting this relationship is to show that when the dispersion of muscle $\dot{V}_{MAX}$ is 0.2 or greater, some regions of muscle will have mitochondrial P_{O_2} values that exceed P_{O_2} of the effluent muscle venous blood.

The role of functional heterogeneities, lung and muscle, on O_2 transport and utilization in healthy subjects at altitude

The four panels in Fig. 5 display the effects of altitude on four key outcome variables at maximal exercise – arterial, muscle venous, and mitochondrial P_{O_2} and $\dot{V}_{O_2max}$ itself. Two relationships are shown in each panel – that computed in the absence of either lung or muscle

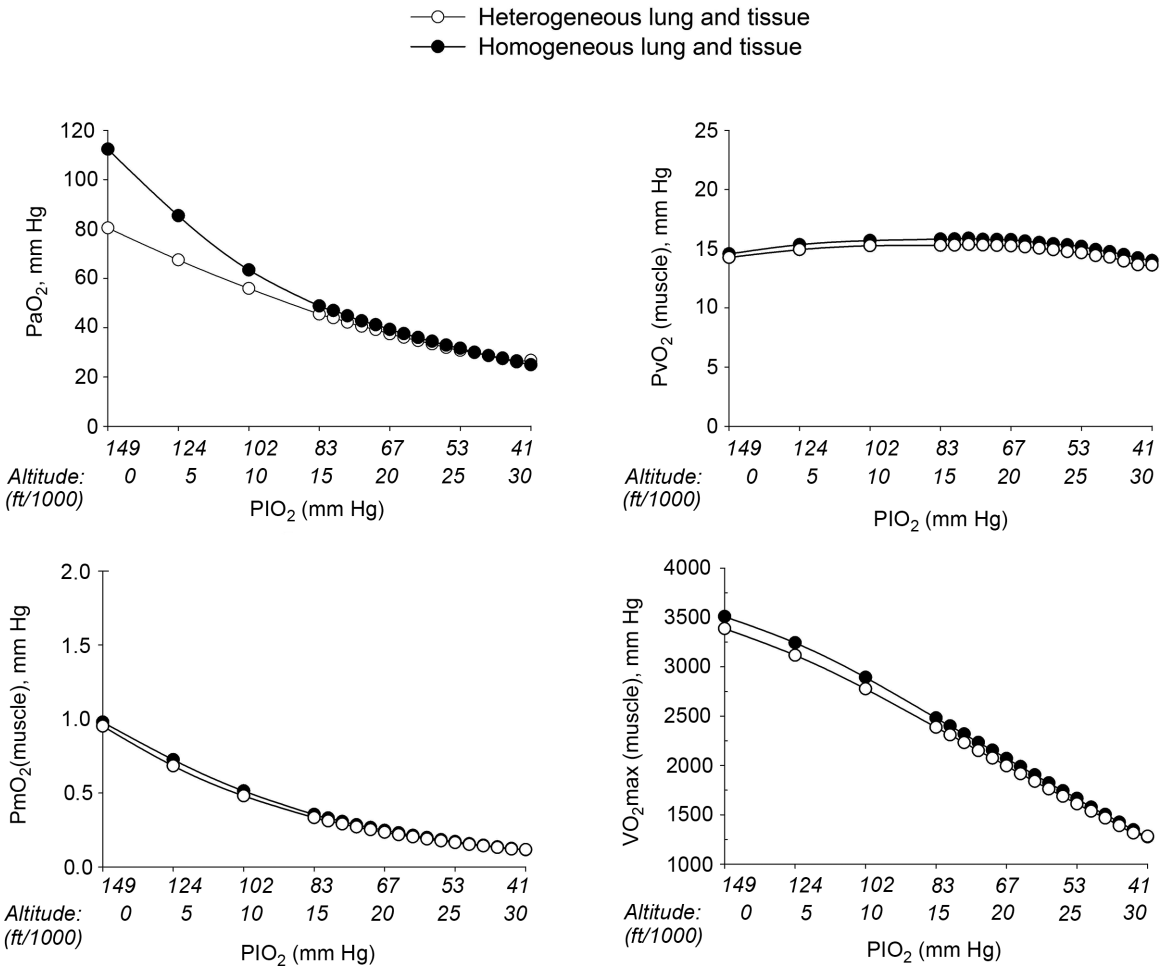

Figure 5. Role of functional heterogeneities, lung and muscle, on the O_2 transport and utilization system in healthy subjects at altitude
Effects of functional inhomogeneity on arterial P_{O_2} (upper left panel), venous P_{O_2} (upper right panel), mitochondrial P_{O_2} (lower left panel) and $\dot{V}_{O_2}$ (lower right panel) at sea level and altitude. Functional inhomogeneity is expressed as the combined effects of lung ventilation–perfusion inequalities and skeletal muscle perfusion–metabolism mismatching. Mitochondrial respiration parameters were fixed to a conservative $\dot{V}_{MAX}$ of 4584 ml min^{-1} and a P_{50} of 0.3 mmHg. Filled circles correspond to simulations outputs when considering both homogeneous lung and tissues. Open circles represent simulation outputs when using reasonable estimates for lung ventilation–perfusion (logSD $\dot{Q}$ of 0.5), tissue perfusion–metabolism (logSD $\dot{V}_{MAX}$ of 0.1), and the metabolic rate of non-exercising tissues (with an assigned $\dot{V}_{O_2}$ of 300 ml min^{-1} and a $\dot{V}_{CO_2}$ of 240 ml min^{-1}) and assuming that 20% of total blood flow goes to non-exercising tissues. See text for details.

heterogeneity, and that computed allowing for reasonable normal estimates of heterogeneity in each location as listed above in the Methods section ($\dot{V}_A/\dot{Q}$ heterogeneity in the lung quantified by a dispersion value (logSD $\dot{Q}$) of 0.5, $\dot{V}_{MAX}/\dot{Q}$ heterogeneity in muscle quantified using an estimate of dispersion (logSD $\dot{V}_{MAX}$) of 0.1, non-exercising body tissues using typical resting total values of $\dot{V}_{O_2}$ (300 ml min^{-1}), $\dot{V}_{CO_2}$ (240 ml min^{-1}) and 20% of total blood flow at peak exercise, and a conservative $\dot{V}_{max}$ value 20% higher than the measured $\dot{V}_{O_2\,max}$). Except for arterial P_{O_2} at sea level and altitudes up to about 10,000 ft, the effects of typical levels of heterogeneity are seen to be small, and diminish progressively with increasing altitude.

Sensitivity of outcomes to mitochondrial respiration and muscle heterogeneity estimates in health

Recall that the three least well established determinants of O_2 flux and partial pressures in the transport–utilization pathway are the $\dot{V}_{MAX}$ and P_{50} of the mitochondrial respiration curve (that links $\dot{V}_{O_2}$ to mitochondrial P_{O_2})

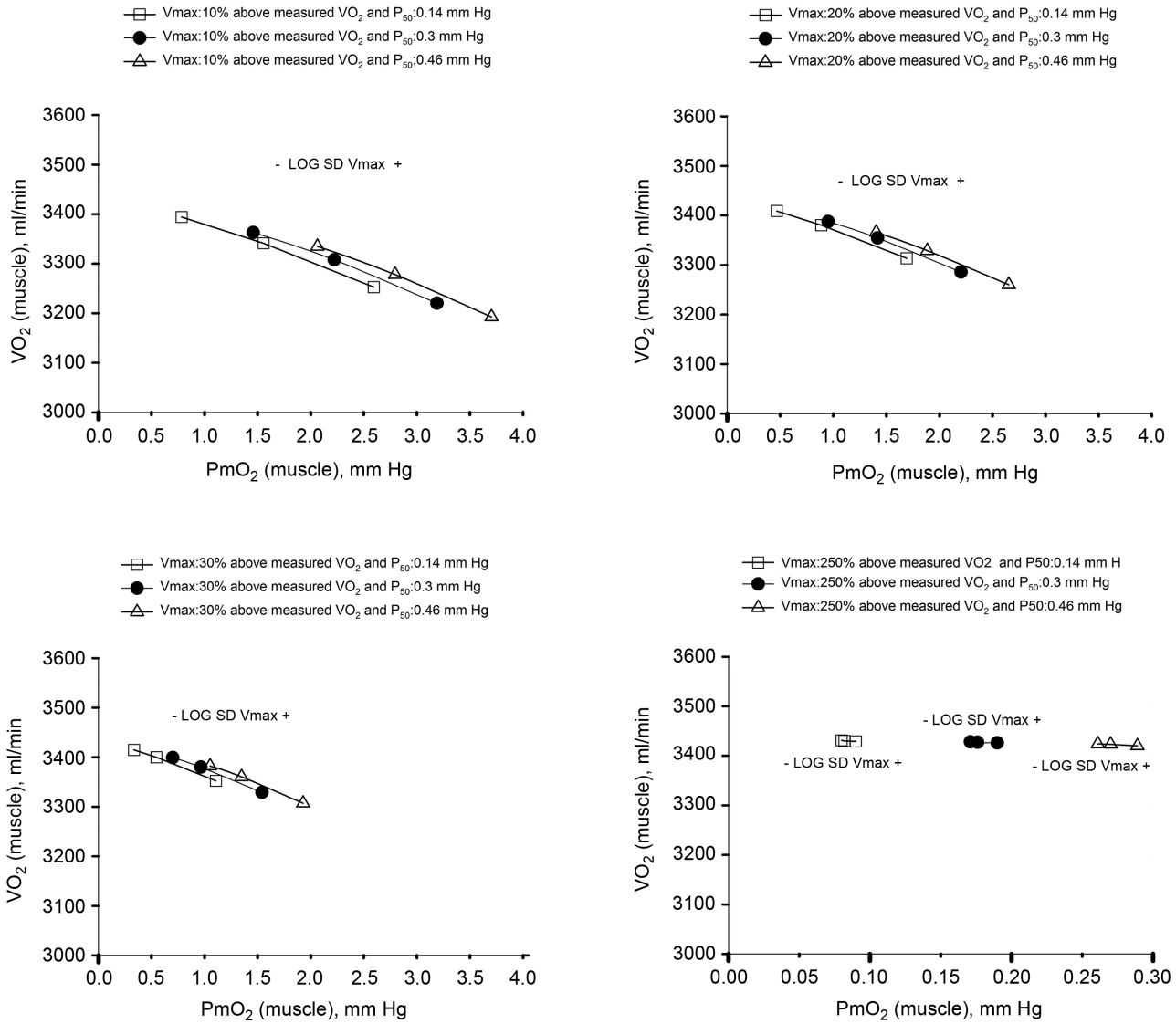

Figure 6. Sensitivity analysis of mitochondrial respiration and muscle heterogeneity estimates in health
Effects of muscle bioenergetics (mitochondrial respiration $\dot{V}_{MAX}$ and P_{50} parameters) and muscle peripheral heterogeneities on muscle $\dot{V}_{O_2}$ and mitochondrial P_{O_2} (P_{mO_2}) in health at sea level. $\dot{V}_{MAX}$ is taken as 10% (upper left panel), 20% (upper right panel), 30% (lower left panel) and 250% (lower right panel) greater than measured $\dot{V}_{O_2\,max}$. For each $\dot{V}_{MAX}$, three mitochondrial P_{50} values (0.14, 0.3 and 0.46 mmHg) and three degrees (0.1, 0.2 and 0.3) of muscle perfusion–metabolism inhomogeneity (logSD $\dot{V}_{MAX}$) were evaluated. See text for details.

and the extent of muscle heterogeneity. Because of this, we carried out calculations of how variation in their assumed values would affect both $\dot{V}_{O_2}$ and mitochondrial P_{O_2} estimates. In this section, we now use (Fig. 6) the four $\dot{V}_{MAX}$ values stated in the Methods section that are 4.2, 4.6, 4.9 and 9.5 l min^{-1}.

For mitochondrial P_{50} (assumed normal value 0.3 mmHg; Wilson *et al.* 1977; Gnaiger *et al.* 1998; Scandurra & Gnaiger, 2010), we also used values of 0.14 and 0.46 mmHg. With heterogeneity of $\dot{V}_{MAX}$ estimated at 0.1 (logSD $\dot{V}_{MAX}$), we also used values of 0.2 (moderate heterogeneity) and 0.3 (severe heterogeneity). This yielded $4 \times 3 \times 3$ or 36 combinations of these variables. It should also be noted that the values chosen reflect substantial relative differences for each variable.

Figure 6 shows the results of this analysis in a format where predicted $\dot{V}_{O_2max}$ is plotted against the corresponding predicted average muscle mitochondrial P_{O_2} so that the effects can be seen for both of these outcome variables. The top panel shows results when $\dot{V}_{MAX} = \dot{V}_{O_2max} + 10\%$; the middle panel for $\dot{V}_{MAX} = \dot{V}_{O_2max} + 20\%$ and the lower panel for $\dot{V}_{MAX} = \dot{V}_{O_2max} + 30\%$. In each panel, open squares represent $P_{50} = 0.14$ mmHg, filled circles a $P_{50} = 0.3$ mmHg and open triangles a $P_{50} = 0.46$ mmHg. For any one such P_{50}, the three connected points in each case reflect, from left to right, logSD $\dot{V}_{MAX} = 0.1$ (normal), 0.2 (moderate), and 0.3 (severe heterogeneity).

In terms of predicted $\dot{V}_{O_2max}$, the consequences of these uncertainties are small. The highest $\dot{V}_{O_2max}$ in all three panels is 3415 ml min^{-1}, and the lowest is 3192 ml min^{-1}. However, in terms of mean mitochondrial P_{O_2}, the effects are greater. P_{mO_2} is systematically higher for the lowest $\dot{V}_{MAX}$ (range of P_{mO_2}: 0.8 to 3.7 mmHg, top panel) to lower panel (highest $\dot{V}_{MAX}$, range of P_{mO_2}: 0.3 to 1.9 mmHg).

In summary, the sensitivity analysis displayed in Fig. 6 points out that at any $\dot{V}_{MAX}$, increase in mitochondrial P_{50} results in systematically higher P_{mO_2} values with almost no effect on the relationship between $\dot{V}_{O_2max}$ and P_{mO_2}. On the other hand, increasing logSD $\dot{V}_{MAX}$ raises average P_{mO_2} for any set of $\dot{V}_{MAX}$ and P_{50} values. Moreover, the figure clearly indicates that the higher the $\dot{V}_{MAX}$, the narrower is the range of potential mitochondrial P_{O_2} values for a given range of logSD $\dot{V}_{MAX}$.

Simulated impact of lung and muscle heterogeneity on P_{mO_2} and muscle $\dot{V}_{O_2}$ in two patients with COPD of different severity: Question 4

As Table 2 shows, lung heterogeneities had been measured in each patient using the multiple inert gas elimination technique (Blanco *et al.* 2010). The first patient displays features that would be regarded as reflecting moderate COPD, while the second patient represents end-stage COPD and extremely limited exercise capacity.

Figure 7 displays the impact of functional lung and muscle heterogeneities on the O_2 pathway in the two COPD patients (moderate severity, left panels and end-stage severity, right panels). The format indicates the values of both predicted $\dot{V}_{O_2max}$ and P_{mO_2} over a range of values of the same three least certain variables ($\dot{V}_{MAX}$ and P_{50} of the mitochondrial respiration curve and degree of muscle $\dot{V}_{MAX}$ heterogeneity, none of which are known for these patients).

The less affected patient (left three panels) behaves in a fashion very similar to that shown in Fig. 6 for normal subjects (other than for absolute values of peak $\dot{V}_{O_2}$ under all conditions). In particular, mitochondrial P_{O_2} values are in the same range as for normal subjects. Variation in P_{mO_2} across muscle regions is considerable (not shown) with a SD of 10 mmHg.

For the severely affected patient (right three panels), peak $\dot{V}_{O_2}$ is insensitive to substantial changes in mitochondrial $\dot{V}_{MAX}$, P_{50} or the extent of heterogeneity. Only mitochondrial P_{50} changes will have some effect on mitochondrial P_{O_2}, but it is important to note that the scale of mitochondrial P_{O_2} is very different than normal, and is far lower under all conditions, with little variation throughout the muscle (SD of 1 mmHg).

Discussion

Summary of major findings

This study has generated the first integrated model of the O_2 pathway that takes into account all the individual components of O_2 transport and utilization considering both exercising and non-exercising tissues at $\dot{V}_{O_2max}$ in health and in disease (i.e. COPD), thus allowing for heterogeneity in both lungs and muscle. A graphical user interface to parameterize and simulate the integrative model is freely available at http://sourceforge.net/projects/o2pathway/.

The research addresses the separate and combined contributions of functional heterogeneities at pulmonary and at skeletal muscle levels to each of the components of the O_2 pathway. Emphasis is placed on estimating the impact of lung and skeletal muscle $\dot{V}_{MAX}/\dot{Q}$ ratio inequalities on overall muscle $\dot{V}_{O_2}$ and on mitochondrial P_{O_2} at maximal exercise. This was done simulating normal subjects at sea level and altitude, and patients with COPD.

The main result from now allowing for lung and muscle heterogeneities is that heterogeneity in muscle affects O_2 availability more than does heterogeneity in the lungs if $\dot{V}_{MAX}$ is only slightly higher than $\dot{V}_{O_2max}$. However, if $\dot{V}_{MAX}$ is greatly in excess of the potential to deliver O_2, as small muscle mass studies suggest (Andersen & Saltin, 1985), the effects of lung and muscle heterogeneity are similar. On the other hand, the impact of lung heterogeneity on $\dot{V}_{O_2max}$ is insensitive to the $\dot{V}_{MAX}$ values used. In addition,

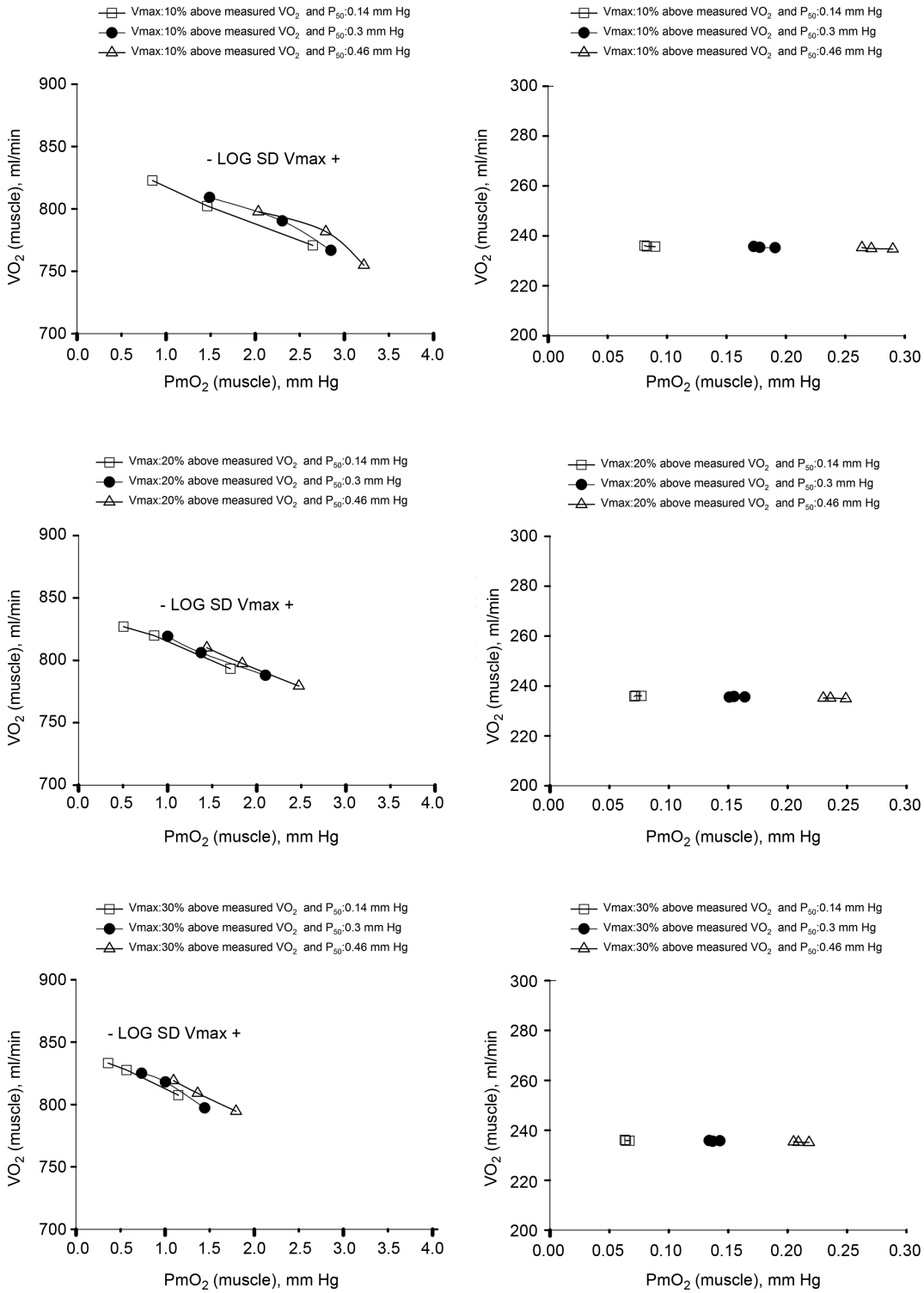

Figure 7. Sensitivity analysis of mitochondrial respiration and muscle heterogeneity estimates in COPD
Effects of muscle bioenergetics (mitochondrial respiration $\dot{V}_{MAX}$ and P_{50} parameters) and muscle peripheral heterogeneities on muscle $\dot{V}_{O_2}$ and mitochondrial P_{O_2} (P_{mO_2}) for given representatives of mild (left-side panels) and severe (right-side panels) limitation of O_2 transport conditions in chronic obstructive pulmonary disease (COPD). $\dot{V}_{MAX}$ is conservatively taken as 10% (upper panels), 20% (middle panels) and 30% (lower panels) greater than measured $\dot{V}_{O_2\,max}$ in the two COPD patients exercising maximally, selected as representatives of both mild and severe O_2 transport conditions. For each $\dot{V}_{MAX}$, three mitochondrial P_{50} values (0.14, 0.3 and 0.46 mmHg) and three degrees (0.1, 0.2 and 0.3) of muscle perfusion–metabolism inhomogeneity (logSD $\dot{V}_{MAX}$) were evaluated. See text for details.

because muscle heterogeneity appears to be less than that in the lung, muscle heterogeneity is predicted to have less of an impact on overall O_2 transport and utilization than observed lung heterogeneity.

These findings stress the need for further measurements of skeletal muscle metabolism–perfusion heterogeneity in health and disease, and also of assessing parameters of the mitochondrial respiration curve ($\dot{V}_{MAX}$ and p_{50}).

Implications of functional heterogeneities: lung and skeletal muscle

Whether arterial oxygenation falls as a result of altitude in normal subjects or as a result of heterogeneity in the lungs in patients with lung disease (at sea level), it is clear that O_2 availability to the muscles must fall. This has been appreciated for many years, as has the consequence of such reduced O_2 availability for maximal exercise capacity. The other potentially important consequence of reduced O_2 availability is reduced mitochondrial P_{O_2}. This may have more than one effect on cellular function.

While heterogeneity in the lungs must cause mitochondrial P_{O_2} to fall throughout the muscle (all other factors unchanged), heterogeneity in the muscles will additionally cause mitochondrial P_{O_2} to vary between muscle regions. In those areas with higher than average $\dot{V}_{MAX}$ in relation to blood flow, mitochondrial P_{O_2} is lower than average, but in regions where $\dot{V}_{MAX}$ is low in relation to blood flow, mitochondrial P_{O_2} must rise to levels greater than would be seen in the absence of heterogeneity. The consequences of subnormal mitochondrial P_{O_2} are discussed below. There may be corresponding functional consequences of a high mitochondrial P_{O_2} as well.

A high P_{O_2} may oppose vasodilatation and restrict local perfusion, thus increasing the $\dot{V}_{MAX}/\dot{Q}$ back towards normal and offering an intrinsic mechanism to automatically limit mitochondrial P_{O_2} heterogeneity. A high mitochondrial P_{O_2} will also reduce the capillary-to-mitochondrial P_{O_2} diffusion gradient, reducing diffusive O_2 transport and again working towards restoring the balance between O_2 supply and demand. Furthermore, the high P_{O_2} may exert genomic effects that may be opposite to those expected when P_{O_2} is below normal (see above). The potential therefore exists for regional regulation of gene expression (and thus for adaptive programs) according to local P_{O_2}. Finally, when mitochondrial P_{O_2} is elevated, the potential exists for increased ROS generation, just as when P_{O_2} is below normal. If so, muscle regions with both very low and very high $\dot{V}_{MAX}/\dot{Q}$ ratios may be at risk of oxidative stress.

Biological and clinical implications

The multilevel impact of disturbances of cellular oxygenation on cell function is well recognized (Semenza, 2011). Hypoxia- (or hyperoxia-) induced biological alterations may play a significant role on underlying mechanisms in different acute and chronic conditions (Resar *et al.* 2005). A major conclusion of the present study is that mitochondrial P_{O_2} will vary considerably among muscle regions of different $\dot{V}_{MAX}/\dot{Q}$ ratio. When $\dot{V}_{MAX}/\dot{Q}$ is low, P_{mO_2} is high, and vice versa. This potential variation in P_{mO_2}, which can occur during exercise in healthy individuals, but can also occur on submaximal exercise or even at rest in severe disease states, may have significant biological implications.

First, since a low P_{O_2} facilitates local vasodilatation in muscle (Rowell, 1986), those areas with high $\dot{V}_{MAX}$ in relation to $\dot{Q}$, thus having a low P_{mO_2}, may preferentially vasodilate, which means that $\dot{Q}$ may increase locally and that the $\dot{V}_{MAX}/\dot{Q}$ ratio is thus, in part, normalized. In this way, $\dot{V}_{MAX}/\dot{Q}$ heterogeneity may be to some extent self-limited. This corresponds to hypoxic pulmonary vasoconstriction in the lungs, where it has been known for many years that a region with a low $\dot{V}_A/\dot{Q}$ ratio will vasoconstrict, limiting blood flow and tending to push the $\dot{V}_A/\dot{Q}$ ratio back towards normal.

Second, the lower the mitochondrial P_{O_2}, the higher will be the P_{O_2} difference between the muscle microvasculature and the mitochondria, other factors being equal. This facilitates the diffusion process, and provides an additional, automatic compensatory mechanism to work in the direction of restoring $\dot{V}_{O_2}$ when blood flow is low. Whether these self-correcting effects are seen in disease remains to be determined.

Potential for estimating P_{mO_2} in health and in disease

It may be possible to measure mitochondrial P_{O_2} (P_{mO_2}) in the future (Mik, 2013) but this promising approach is not yet generally available. If this, or another, method can be developed into a feasible approach for intact humans, it offers the potential for estimating, at least approximately, the parameters of the *in vivo* mitochondrial O_2 respiration curve. By varying inspired O_2 concentration over as wide a range as safely possible, paired values of $\dot{V}_{O_2}$ and P_{mO_2} could be measured, and if they were to bracket both the O_2-dependent and O_2-independent regions of the mitochondrial respiration curve, there may be enough information to estimate $\dot{V}_{MAX}$and P_{50}.

Limitations of the analysis

Firstly, as in previous work (Wagner, 1993, 1996; Cano *et al.* 2013), the entire analysis applies to steady-state conditions (meaning, that O_2 partial pressures are constant in time, as is $\dot{V}_{O_2}$ itself). Therefore, the analyses should not be extrapolated to transient changes in metabolic rate at the beginning or end of exercise.

Additional limitations are that for this modelling approach to apply with accuracy, parameters defining the *in vivo* mitochondrial respiration curve ($\dot{V}_{MAX}$ and P_{50}), and muscle diffusing capacity (DM), are required. Indeed, as already stated in Methods, section headed 'Analysis and input data for simulations', data from experimental human exercise studies do not exist for $\dot{V}_{max}$ and P_{50}. In addition, our vision was to explore heterogeneities between relatively large skeletal muscle regions (on a scale of cm^3) that can be explored in humans by methods such as PET (Nuutila & Kalliokoski, 2000) or NIRS (Vogiatzis *et al.* 2015). At $\dot{V}_{O_2max}$, tissue P_{O_2} has wide spatial variations within the region surrounding each individual capillary, due both to axial gradients in intravascular oxygen levels and to radial gradients of tissue oxygen levels (Weibel, 1984; McGuire & Secomb, 2001). Consequently, large variations in mitochondrial P_{O_2} (from values below 1 mmHg up to double-digit P_{O_2} values (McGuire & Secomb, 2001)) exist within any region of a size that can be resolved with techniques that are feasible in humans. Hence, P_{mO_2} in Fig. 1 (eqn (5)) can be regarded as an effective or average value over such a region of observation. More detailed consideration of the spatial structure of the microcirculation would be needed to overcome this limitation of the model (Duling & Damon, 1987; Delashaw & Duling, 1988).

In addition, while the degree of $\dot{V}_A/\dot{Q}$ heterogeneity in the lungs of individual subjects or patients has been measurable for many years, that in the muscle is not easily accessible. Thus, for the present paper, the estimates used are uncertain, and the quantitative outcomes should not be generalized – they are specific to the particular input variables we used. That is why we elected to run simulations over a range of the most uncertain variables. That said, given that the principal objective of our study was to present the development of an O_2 transport model that encompasses heterogeneity in both lungs and muscle, it seems reasonable to illustrate its prediction capabilities, even if estimates of some input variables are uncertain (i.e. DM, $\dot{V}_{MAX}$, P_{50}). With the algorithm now developed, running the simulations with accurate data when available will easily be possible. The quantitative results presented thus show the impact of heterogeneity only for the specific cases simulated.

Conclusions

The current research incorporates functional heterogeneities in lung and muscle, as well as the O_2 consumed by non-exercising tissues, into a previously established integrative O_2 pathway mathematical model that had considered both the lungs and muscles as functionally homogeneous, and which also ignored O_2 consumed by non-exercising tissues. These modifications allow application of the modelling approach to patients with impaired exercise capacity and cardio-pulmonary diseases such as COPD. Skeletal muscle $\dot{V}_{MAX}/\dot{Q}$ ratio inequality is predicted to lead to impaired muscle performance and low mitochondrial P_{O_2} in high $\dot{V}_{MAX}/\dot{Q}$ ratio muscle compartments, and excess oxygen availability and high mitochondrial P_{O_2} in low $\dot{V}_{MAX}/\dot{Q}$ ratio compartments. Such changes in mitochondrial P_{O_2} might in turn affect regional vasomotor control, reactive O_2 species generation, and possibly gene expression.

References

Andersen P & Saltin B (1985). Maximal perfusion of skeletal muscle in man. *J Physiol* **366**, 233–249.

Blanco I, Gimeno E, Munoz PA, Pizarro S, Gistau C, Rodriguez-Roisin R, Roca J & Barberà JA (2010). Hemodynamic and gas exchange effects of sildenafil in patients with chronic obstructive pulmonary disease and pulmonary hypertension. *Am J Respir Crit Care Med* **181**, 270–278.

Cano I, Mickael M, Gomez-Cabrero D, Tegnér J, Roca J & Wagner PD (2013). Importance of mitochondrial in maximal O_2 transport and utilization: A theoretical analysis. *Respir Physiol Neurobiol* **189**, 477–483.

Delashaw JB & Duling BR (1988). A study of the functional elements regulating capillary perfusion in striated muscle. *Microvasc Res* **36**, 162–171.

Duling BR & Damon DH (1987). An examination of the measurement of flow heterogeneity in striated muscle. *Circ Res* **60**, 1–13.

Gnaiger E, Lassnig B, Kuznetsov A, Rieger G & Margreiter R (1998). Mitochondrial oxygen affinity, respiratory flux control and excess capacity of cytochrome c oxidase. *J Exp Biol* **201**, 1129–1139.

Hammond MD & Hempleman SC (1987). Oxygen diffusing capacity estimates derived from measured VA/Q distributions in man. *Respir Physiol* **69**, 129–147.

Kelman GR (1966). Digital computer subroutine for the conversion of oxygen tension into saturation. *J Appl Physiol* **21**, 1375–1376.

Knight DR, Poole DC, Schaffartzik W, Guy HJ, Prediletto R, Hogan MC & Wagner PD (1992). Relationship between body and leg $\dot{V}_{O_2}$ during maximal cycle ergometry. *J Appl Physiol (1985)* **73**, 1114–1121.

McGuire BJ & Secomb TW (2001). A theoretical model for oxygen transport in skeletal muscle under conditions of high oxygen demand. *J Appl Physiol (1985)* **91**, 2255–2265.

Mik EG (2013). Measuring mitochondrial oxygen tension: from basic principles to application in humans. *Anesth Analg* **117**, 834–846.

Nuutila P & Kalliokoski K (2000). Use of positron emission tomography in the assessment of skeletal muscle and tendon metabolism and perfusion. *Scand J Med Sci Sports* **10**, 346–350.

Resar JR, Roguin A, Voner J, Nasir K, Hennebry TA, Miller JM, Ingersoll R, Kasch LM & Semenza GL (2005). Hypoxia-inducible factor 1α polymorphism and coronary collaterals in patients with ischemic heart disease. *Chest* **128**, 787–791.

Richardson RS, Haseler LJ, Nygren AT, Bluml S & Frank LR (2001). Local perfusion and metabolic demand during exercise: a noninvasive MRI method of assessment. *J Appl Physiol (1985)* **91**, 1845–1853.

Rowell LB (1986). Cardiovascular adjustments to hypoxemia. In *Human Circulation: Regulation during Physical Stress*, pp. 329–361. Oxford University Press, New York.

Scandurra FM & Gnaiger E (2010). Cell respiration under hypoxia: facts and artefacts in mitochondrial oxygen kinetics. *Adv Exp Med Biol* **662**, 7–25.

Semenza GL (2011). Oxygen sensing, homeostasis, and disease. *N Engl J Med* **365**, 537–547.

Sutton JR, Reeves JT, Wagner PD, Groves BM, Cymerman A, Malconian MK, Rock PB, Young PM, Walter SD & Houston CS (1988). Operation Everest II: oxygen transport during exercise at extreme simulated altitude. *J Appl Physiol* **64**, 1309–1321.

Vogiatzis, I, Habazettl H, Louvaris Z, Andrianopoulos V, Wagner H, Zakynthinos S, Wagner PD (2015). A method for assessing heterogeneity of blood flow and metabolism in exercising normal human muscle by near infrared spectroscopy. *J Appl Physiol* **118**(in press), doi: 10.1152/japplphysiol.00458.2014.

Wagner PD (1993). Algebraic analysis of the determinants of $\dot{V}_{O_2max}$. *Respir Physiol* **93**, 221–237.

Wagner PD (1996). A theoretical analysis of factors determining $\dot{V}_{O_2max}$ at sea level and altitude. *Respir Physiol* **106**, 329–343.

Wagner PD (2008). The multiple inert gas elimination technique (MIGET). *Intensive Care Med* **34**, 994–1001.

Wagner PD, Hedenstierna G & Bylin G (1987*a*). Ventilation-perfusion inequality in chronic asthma. *Am Rev Respir Dis* **136**, 605–612.

Wagner PD, Laravuso RB, Uhl RR & West JB (1974). Continuous distributions of ventilation-perfusion ratios in normal subjects breathing air and 100 per cent O_2. *J Clin Invest* **54**, 54–68.

Wagner PD, Sutton JR, Reeves JT, Cymerman A, Groves BM & Malconian MK (1987b). Operation Everest II: pulmonary gas exchange during a simulated ascent of Mt Everest. *J Appl Physiol (1985)* **63**, 2348–2359.

Weibel, ER (1984). *The Pathway for Oxygen*. Harvard University Press, Cambridge, MA, USA.

Welch HG (1982). Hyperoxia and human performance: a brief review. *Med Sci Sports Exerc* **14**, 253–262.

West JB (1969). Ventilation–perfusion inequality and overall gas exchange in computer models of the lung. *Respir Physiol* **7**, 88–110.

West JB (1971). Causes of carbon dioxide retention in lung disease. *N Engl J Med* **284**, 1232–1236.

Wilson DF, Erecinska M, Drown C & Silver IA (1977). Effect of oxygen tension on cellular energetics. *Am J Physiol Cell Physiol* **233**, C135–C140.

Additional information

Competing interests

No competing interests.

Author contributions

I.C., J.R. and P.D.W. made substantial contributions to conception and design, and/or acquisition of data, and/or analysis and interpretation of data; I.C. and P.D.W. constructed, tested and run the algorithms used in the model; I.C., J.R. and P.D.W. participated in drafting the article and revising it critically for important intellectual content and gave final approval of the version to be submitted and any revised version.

Funding

This research has been carried out under the Synergy-COPD research grant, funded by the Seventh Framework Program of the European Commission as a Collaborative Project with contract no.: 270086 (2011–2014), and NIH P01 HL091830.